Cardiovascular Research (2016) **109**, 294–304
doi:10.1093/cvr/cvv241

Enhanced atheroprotection and lesion remodelling by targeting the foam cell and increasing plasma cholesterol acceptors

Se-Hee Son[1†], Young-Hwa Goo[1†], Mihyun Choi[1], Pradip K. Saha[2], Kazuhiro Oka[2], Lawrence C. B. Chan[2], and Antoni Paul[1*]

[1]Center for Cardiovascular Sciences, Albany Medical College, 47 New Scotland Avenue, MC-8, Albany, NY 12208, USA; and [2]Division of Diabetes, Endocrinology and Metabolism, Department of Medicine, Baylor College of Medicine, Houston, TX, USA

Received 1 April 2015; revised 29 September 2015; accepted 6 October 2015; online publish-ahead-of-print 20 October 2015

Time for primary review: 33 days

Aims Atherosclerosis development can be ameliorated by promoting reverse cholesterol transport (RCT) from arteries. The process involves cholesterol efflux from foam cells to extracellular acceptors such as apolipoprotein A-I (apoA-I) and high-density lipoprotein (HDL) that mediate transport to the liver. Perilipin-2 (PLIN2) is a lipid droplet (LD)-associated protein that in macrophages facilitates cholesterol storage and prevents efflux. We hypothesized that atheroprotection would be enhanced by concurrently targeting PLIN2 to increase the efflux capacity of foam cells and increasing plasma apoA-I and HDL.

Methods and results PLIN2-knockout and wild-type mice lacking apolipoprotein E (PLIN2$^{-/-}$/apoE$^{-/-}$ and PLIN2$^{+/+}$/apoE$^{-/-}$) were treated with a helper-dependent adenoviral vector encoding human apoA-I (HDAd-AI) or with control empty vector. Treatment with HDAd-AI increased hepatic apoA-I production, plasma apoA-I and HDL-cholesterol (HDL-C), and apoA-I deposition in lesions to a similar extent in PLIN2$^{-/-}$/apoE$^{-/-}$ and PLIN2$^{+/+}$/apoE$^{-/-}$ mice. However, atherosclerosis development at the aortic sinus was considerably lower in HDAd-AI-treated PLIN2$^{-/-}$/apoE$^{-/-}$ mice. A more stable lesion phenotype, with increased collagen content, was primarily associated to treatment with HDAd-AI, but was enhanced under PLIN2 deficiency. PLIN2 deficiency and apoA-I cumulatively reduced LDs and cholesterol ester content in cultured macrophages. Neutral lipid in atheroma was significantly reduced in HDAd-AI-treated PLIN2$^{-/-}$/apoE$^{-/-}$ mice, and RCT from macrophages to feces was enhanced in PLIN2$^{-/-}$ macrophages.

Conclusion These studies demonstrate a mutually beneficial relationship between PLIN2 deficiency and elevated apoA-I/HDL-C in preventing atherosclerosis development. The data support that targeting foam cell components to mobilize cholesterol may be a promising strategy to enhance the atheroprotection of plasma cholesterol acceptors.

Keywords Apolipoprotein A-I • Atherosclerosis • Foam cell • Lipid droplet • Perilipin-2 • Reverse cholesterol transport

1. Introduction

The lipid laden macrophage, or foam cell, plays a central role in the regulation of cholesterol deposition at the arterial wall.[1] Arterial macrophages internalize modified low-density lipoprotein particles in an unfettered fashion and retain a significant amount of lipoprotein-derived cholesterol stored as cholesterol ester (CE) within a plethora of cytoplasmic lipid droplets (LDs).[2] LDs consist of a hydrophobic core of neutral lipid, primarily CE in foam cells, coated and stabilized within the aqueous cytoplasm by a monolayer of phospholipids and free cholesterol, and by a number of LD-associated proteins. The main protein coating LDs of macrophages/foam cells is perilipin 2 (PLIN2), also known as adipose differentiation related protein (abbreviated ADFP or ADRP) and adipophilin (human) before a unified nomenclature for the family members was adopted.[2,3] PLIN2 levels increase very significantly upon lipid loading, in part because lipids induce its expression and in part because the protein is stabilized when bound to LDs.[4] Hence, PLIN2 can be used as a marker of intracellular lipid loading, and for the diagnosis of diseases associated with lipid deposition in tissues.[5] In addition, PLIN2 has been shown to play a functional role in the regulation of lipid accumulation in various tissues such as liver, skeletal muscle, retina, and sebaceous gland.[6–9] In cultured macrophages,

* Corresponding author. Tel: +1 518 262 1158; fax: +1 518 262 8101, E-mail: paula@mail.amc.edu

† These authors contributed equally to this manuscript.

PLIN2 up-regulation and down-regulation increased and decreased, respectively, cytoplasmic LD accumulation and, consequently, CE stores.[2,10,11] Interestingly, the rate of cholesterol efflux was decreased by PLIN2 up-regulation and increased by PLIN2 depletion, suggesting that storage within LDs hinders cholesterol efflux.[2,10] Previously we showed that genetic disruption of PLIN2 reduced the number of LDs in foam cells resident within mouse atherosclerotic lesions, that PLIN2 deficiency is well-tolerated by the macrophage, and that atherosclerosis development was attenuated in PLIN2-deficient (PLIN2$^{-/-}$) mice.[2,11]

The cholesterol effluxed by foam cells is taken over by extracellular acceptors that mediate reverse transport (RCT) to the liver for excretion in the bile and ultimately the feces.[12] The main cholesterol acceptors are high-density lipoprotein (HDL) and free apolipoprotein A-I (apoA-I). Upon lipidation, apoA-I forms nascent HDL particles, and apoA-I is the most abundant protein component in HDL.[13] Epidemiological studies have shown a strong inverse correlation between plasma levels of apoA-I and HDL-cholesterol (HDL-C) and the risk of cardiovascular disease.[14] Supporting the epidemiological data, a fair number of studies in animal models have shown protection against atherosclerosis following increases in plasma apoA-I and HDL-C.[15–20] Here we hypothesized that implicit in a scenario where atheroprotection can be achieved by increasing either the ability of the foam cell to efflux cholesterol or the capacity of plasma to accept and transport it, is the possibility that the efficacy of targeting foam cell proteins might be limited by the level of extracellular cholesterol acceptors and that, accordingly, cholesterol retention within foam cells may limit the atheroprotection mediated by plasma cholesterol acceptors. ApoA-I is mainly synthesized by the liver, and a lifetime increase in plasma apoA-I can be safely achieved by helper-dependent adenovirus (HDAd)-mediated gene transfer.[19,21] Thus, we compared the effect on atherosclerosis development of PLIN2 deficiency alone, of treatment with a HDAd encoding the human apoA-I gene (HDAd-AI), or the combination of both factors. The data presented in this manuscript support a mutually beneficial relationship between PLIN2 inactivation and elevated plasma apoA-I and HDL-C in preventing arterial lipid deposition and atherosclerosis development, and in the development of a more stable lesion phenotype.

2. Materials and methods

2.1 Animal studies

Littermate PLIN2$^{+/+}$/apoE$^{-/-}$ and PLIN2$^{-/-}$/apoE$^{-/-}$ female mice were generated from PLIN2$^{+/-}$/apoE$^{-/-}$ breeding pairs.[2] At 8 weeks of age, blood was drawn for baseline plasma measurements, and 11–12 mice of each genotype were injected with a single dose of 7.5×10^{12} vector particles/kg of either HDAd-AI or control empty vector (HDAd-0). HDAds were injected via retro-orbital venous sinus to mice anaesthetized with ketamine (100 mg/kg) and xylazine (10 mg/kg), administered intraperitoneally. Body weights and plasma lipids were monitored at 11 weeks and 20 weeks of age. Mice were fed standard chow throughout the study. Mice were sacrificed at 20 weeks by exsanguination under anaesthesia with ketamine and xylazine. The study was conducted in accordance with the NIH Guide for the Care and Use of Laboratory Animals, following protocols approved by the Institutional Animal Care and Use Committee at Albany Medical College.

2.2 Production of HDAd-AI vector

An 11-kb *Eco*RI fragment containing the human apoA-I gene was cloned into an HDAd vector (see Supplementary material online, *Figure S1*). The vector was generated, amplified, and characterized at the Gene Vector Core at Baylor College of Medicine as previously described.[19,21]

2.3 Analysis of atherosclerotic lesions

Cross-sections of the aortic sinus were stained with oil red O. Lesion area was determined in six sections spanning the region from the very proximal aorta to the point that contains three complete leaflets by outlining the area between the media layer and the vessel lumen following the method of Dr Paigen as we previously described.[2,22] Immunohistochemistry was performed using primary antibodies against apoA-I (Santa Cruz Biotechnology) and a macrophage marker (Mac-3/LAMP-2, Santa Cruz Biotechnology).[2,23] Oil red O and Masson's trichrome stainings were performed using standard protocols. Neutral lipid staining with the fluorescent dye BODIPY 493/503 (Life Technologies) was performed following the manufacturer's instructions. The intensities and/or areas of staining were determined using Image J and AxioVision (Carl Zeiss Microscopy) softwares.

2.4 Plasma and liver analyses

Total plasma cholesterol and HDL-C were measured using the Wako Cholesterol E and HDL-Cholesterol E kits, respectively. Plasma triglycerides were measured with Infinity™ Triglycerides (Thermo Scientific). Plasma concentrations of human apoA-I were determined using an ELISA kit from MABTECH. Immunoblots to detect total apoA-I (mouse + human) were performed with an antibody from Santa Cruz Biotechnology. An antibody from Calbiochem was used to specifically detect human apoA-I. At the final time point, lipoproteins in plasma pools of each experimental group were fractionated by fast performance liquid chromatography (FPLC) as previously described.[2] The hepatic levels of mouse and human apoA-I mRNA were determined by quantitative real-time PCR (qPCR) using cyclophilin A to normalize values. Primers are listed in Supplementary material online, *Table S1*.

2.5 Experiments in cultured macrophages

Thioglycollate-elicited peritoneal macrophages (PM) from were isolated from PLIN2$^{+/+}$ and PLIN2$^{-/-}$ mice in C57BL6/J background that were anaesthetized with 5% isoflurane and sacrificed by cervical dislocation. Macrophages were cultured in DMEM-0.2% BSA containing acetylated low-density lipoprotein (acLDL, 50 μg/mL, Biomedical Technologies) for 24 h, washed, and incubated for an additional 24 h in DMEM-0.2% BSA or in DMEM-0.2% BSA supplemented with apoA-I (10 μg/mL, Biomedical Technologies). To calculate the total area of LDs and the size distribution of LDs, PM were stained with oil red O and counterstained with Harris Haematoxylin, and the perimeters of individual LDs in 11–15 cells per treatment group were outlined using the AxioVision software (Carl Zeiss Microimaging). To measure intracellular CE, macrophages were cultured in DMEM-0.2% BSA containing acLDL (50 μg/mL) labelled with [1α, 2α(N)-^{3}H]-cholesterol for 24 h, thoroughly washed, and cultured in DMEM-0.2% BSA or in DMEM-0.2% BSA supplemented with apoA-I (10 μg/mL) for an additional 24 h. Lipid and protein were extracted, lipids were resolved by TLC, and the amount of ^{3}H-labelled CE was determined by scintillation counting and normalized to protein.[23] RNA was isolated from PM cultured in the absence of acLDL, or treated with acLDL for 24 h and cultured for an additional 6 h with or without apoA-I. The expression of several genes involved in cholesterol trafficking was determined by qPCR and normalized to cyclophilin A. Primers are listed in Supplementary material online, *Table S1*.

2.6 *In vivo* macrophage-to-feces RCT assay

Thioglycollate-elicited PM were isolated from PLIN2$^{+/+}$/apoE$^{-/-}$ and PLIN2$^{-/-}$/apoE$^{-/-}$ mice. For radioactive labelling, PM were incubated with DMEM-0.2% BSA containing 50 μg/mL acLDL and 5 μCi/mL ^{3}H-cholesterol for 24 h. Cells were extensively washed, equilibrated for 4 h in DMEM-0.2% BSA, and resuspended in ice-cold PBS. For *in vivo* RCT assays, $\sim 2 \times 10^6$ PM were injected intraperitoneally into individually housed apoE$^{-/-}$ mice previously treated with HDAd-AI. Recipients were randomly distributed into two groups that received either

WT or PLIN2$^{-/-}$ PM. Blood was obtained via tail vein bleeding at 5, 24, and 48 h of PM injection, and an aliquot of plasma was used for liquid scintillation counting. Feces were continuously collected for 48 h, homogenized in 50% NaOH overnight, and an aliquot used for liquid scintillation counting. At 48 h, mice were sacrificed by cervical dislocation under anaesthesia with 5% isoflurane; livers were collected and weighted; and 0.3 g of tissue was solubilized in SOLVABLE™ (Perkin Elmer) and the radioactivity determined by scintillation counting. RCT to plasma, feces, and liver was calculated as a percentage of total radioactivity injected at baseline.[24,25]

2.7 Data analysis

Two-way ANOVA was used for multiple comparisons on the effects of the variables PLIN2 genotype and extracellular acceptors. *Post hoc* pairwise comparisons were performed using the Tukey's test. Statistical analyses of experiments involving only two groups were performed using a two-tailed Student' *t*-test. Differences were considered significant at $P < 0.05$. Data are shown as mean ± SEM.

3. Results

3.1 Effect of PLIN2 deficiency and apoA-I on macrophage LD content and CE stores

To determine how PLIN2 ablation, high levels of cholesterol acceptors, and the combination of both factors affect cytoplasmic lipid stores, we incubated WT and PLIN2$^{-/-}$ PM with acLDL (50 μg/mL) for 24 h in media poor in acceptors (DMEM-0.2% BSA), removed the acLDL from the culture media, and incubated the cells in DMEM-0.2% BSA or in DMEM-0.2% BSA supplemented with apoA-I (10 μg/mL) for an additional 24 h. As seen in *Figure 1A*, in response to cholesterol loading with acLDL, the cytoplasm of WT macrophages cultured in the absence of acceptors was abundant with LDs. Both PLIN2 deficiency and treatment with apoA-I significantly reduced the area of cytoplasm covered by LDs (*Figure 1A* and *B*). Whereas lack of PLIN2 reduced the number of cytoplasmic LDs of all sizes, treatment with apoA-I did not affect the number of small LDs of <1 μm^2. However, it significantly

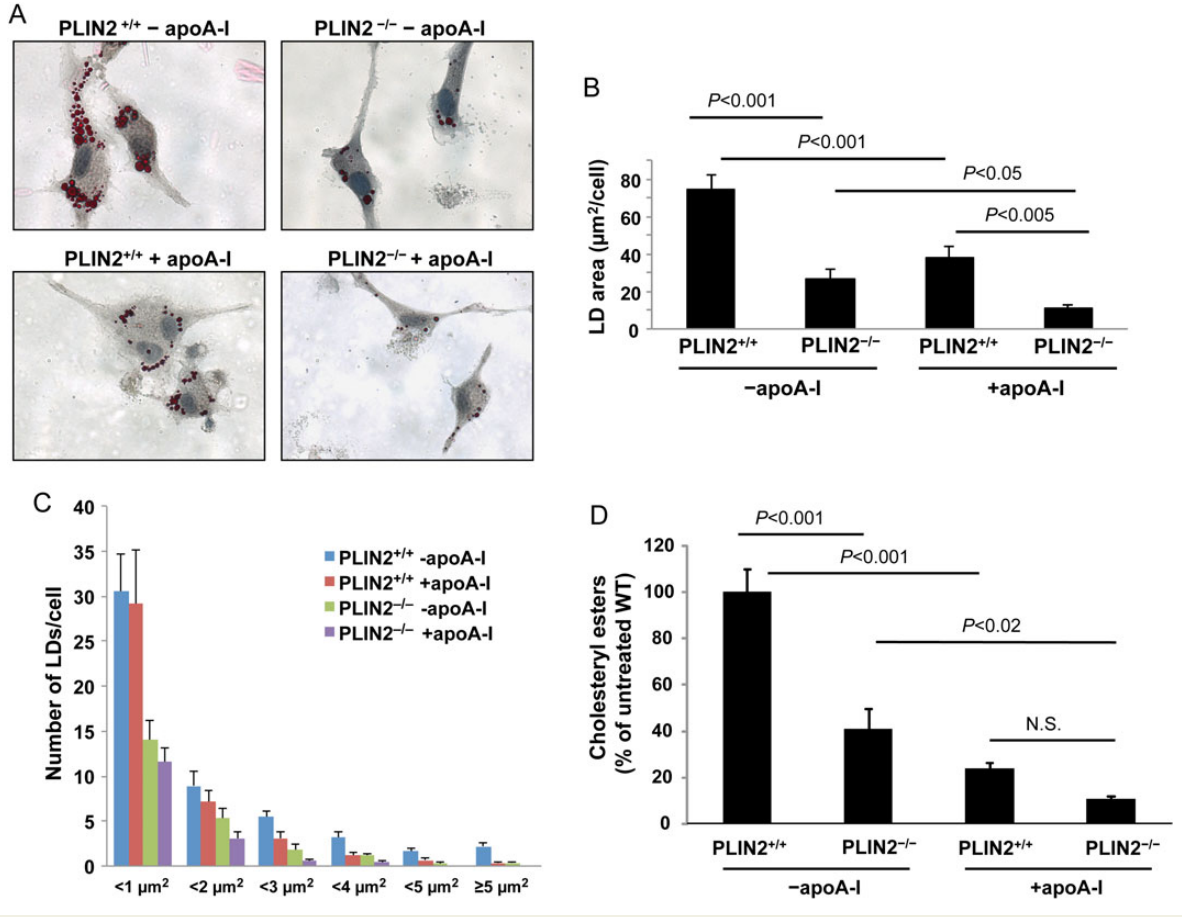

Figure 1 PLIN2 deficiency and apoA-I cooperatively reduced cytoplasmic LDs and CE accumulation. (*A*) Representative images of oil red O-stained PM isolated from PLIN2$^{+/+}$ and PLIN2$^{-/-}$ mice. Macrophages were cholesterol loaded by treatment with acLDL (50 μg/mL) for 24 h and cultured for an additional 24 h in media that was either poor in acceptors (−apoA-I) or was supplemented with 10 μg/mL of apoA-I (+apoA-I). (*B* and *C*) the total oil red O-stained area (*B*) and the size distribution of the LDs (*C*) were determined in 11–15 cells per group. (*D*) CE content in cholesterol-loaded PM cultured under the same conditions described above. ($n = 4$). Two-way ANOVA showed that both PLIN2 genotype and apoA-I significantly influence the area of LDs ($P < 0.001$ for each factor) and CE content ($P < 0.001$ for each factor). The *P*-values of pairwise comparisons within each factor are shown in the plots.

reduced the number of larger LDs and the overall average LD size (*Figure 1A* and *C* and see Supplementary material online, *Figure S2*).

To assess whether the changes in LD number and/or size would be reflected in changes in CE content, as expected given that CE is stored in the core of LDs, we cultured PM in media containing acLDL labelled with ^{3}H-cholesterol. Following cholesterol loading and culture with or without apoA-I supplementation for the same time periods indicated above, lipids were resolved by TLC, and the radioactivity in the CE bands was measured by scintillation counting and normalized to protein. As seen in *Figure 1D*, individually both PLIN2 deficiency and extracellular apoA-I significantly reduced intracellular CE content but, in harmony with the LD measurements, CE content was lower in PLIN2$^{-/-}$ PM cultured with apoA-I. Gene expression analyses did not show differences in the expression of other main players in cholesterol trafficking in macrophages (see Supplementary material online, *Figure S3*). These results are in agreement with previous reports that showed that changes in cholesterol homeostasis upon PLIN2 up-regulation or down-regulation took place in the absence of changes in the expression of genes involved in lipid uptake or efflux.[2,10] Thus, the impact of the combination of PLIN2 deficiency and apoA-I on LD and CE content in cultured PM was higher than the individual impacts of PLIN2 deficiency and treatment with apoA-I. Next, we asked how the combination of these two factors would affect atherosclerosis development.

3.2 *In vivo* generation of apoA-I and HDL-C, and apoA-I deposition in lesions

Previously we showed that PLIN2 deficiency protects both male and female apoE$^{-/-}$ mice against atherosclerosis development. We also observed a similar degree of atheroprotection under global PLIN2 deficiency and in mice lacking PLIN2 only in bone marrow-derived cells. Thus, to study the interrelationship between PLIN2 and circulating cholesterol acceptors during atherosclerosis development *in vivo*, we used a HDAd vector system for hepatic delivery of the human apoA-I gene to female PLIN2$^{+/+}$/apoE$^{-/-}$ and PLIN2$^{-/-}$/apoE$^{-/-}$ mice.[2] The study design is summarized in *Figure 2A*. Because HDAd vectors lack the coding sequences necessary for replication, they can be used *in vivo* with negligible toxicity, and a single dose of vector can lead to lifetime expression of the transgene.[21] Mice were injected with either HDAd-AI or control empty vector (HDAd-0) at 8 weeks of age, and the presence of human ApoA-I in plasma was tested by immunoblotting 3 weeks post-injection. As seen in *Figure 2B*, human apoA-I was readily detectable at this time point, and the expression of human apoA-I considerably increased the total levels of circulating apoA-I. Plasma apoA-I remained elevated through the end of the study, and both human and total apoA-I levels were similar between PLIN2$^{+/+}$/apoE$^{-/-}$ and PLIN2$^{-/-}$/apoE$^{-/-}$ mice (*Figure 2B*). ELISA quantification of human apoA-I in plasma at the end of the study also yielded comparable values between mice that did or did not express PLIN2: 156 $\pm$ 13 mg/dL in PLIN2$^{+/+}$/apoE$^{-/-}$ mice and 128 $\pm$ 21 mg/dL in PLIN2$^{-/-}$/apoE$^{-/-}$ mice (*Figure 2C*). These values lay within the normal range of plasma apoA-I concentrations observed in humans.[26] Human and mouse apoA-I mRNA levels in liver determined at the time of sacrifice were also similar between mice that did or did not express PLIN2 (*Figure 2D* and *E*). Production of human apoA-I did not alter mouse apoA-I mRNA levels (*Figure 2D* and *E*). At the protein level, total apoA-I in liver lysates was also similarly elevated in HDAd-AI-treated mice of both genotypes (*Figure 2F*).

Treatment with HDAd-AI significantly increased plasma HDL-C by ~2.5-fold, from average concentrations that ranged between 27 and 39 mg/dL before treatment and in HDAd-0-treated mice, to

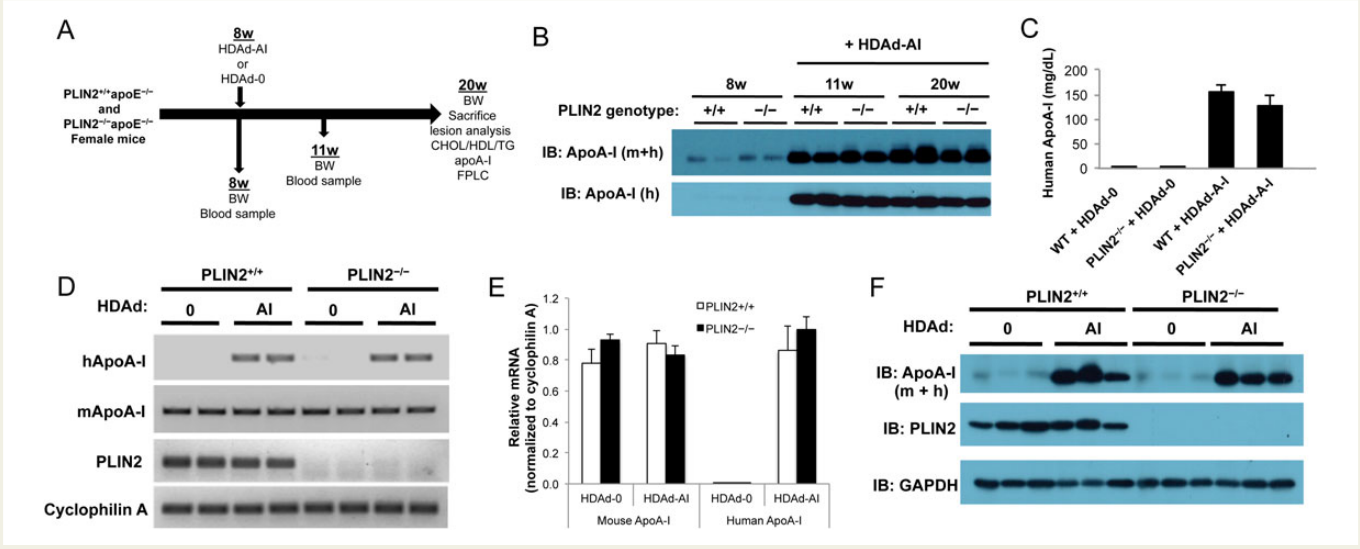

Figure 2 Study design and HDAd-AI-mediated expression of apoA-I. (*A*) Schematic representation of the study design. (*B*) Immunoblots on plasma samples were performed with antibodies that recognize human (h) and total (mouse + human, m + h) apoA-I. PLIN2$^{+/+}$/apoE$^{-/-}$ (+/+) and PLIN2$^{-/-}$/apoE$^{-/-}$ (−/−) mice were bled before and after HDAd-AI injection (+HDAd-AI). While the figure displays representative examples, analysis of plasma samples from all mice included in the study yielded similar results. (*C*) ELISA quantification of plasma human apoA-I at the time of sacrifice (n = 11–12). (*D* and *E*) Relative RT-PCR analysis (29 cycles) (*D*) and qPCR analysis (n = 6) relative to cyclophilin A (*E*) of hepatic mouse and human apoA-I mRNA expression in PLIN2$^{+/+}$/apoE$^{-/-}$ and PLIN2$^{-/-}$/apoE$^{-/-}$ mice that were treated with HDAd-AI or with control empty vector (HDAd-0). (*F*) Immunoblots performed on liver protein lysates of PLIN2$^{+/+}$/apoE$^{-/-}$ and PLIN2$^{-/-}$/apoE$^{-/-}$ mice treated with HDAd-AI or with HDAd-0 (n = 3).

~90 mg/dL (*Figure 3A* and see Supplementary material online, *Table S2*). HDL-C levels were similar between mice that did or did not express PLIN2 at all time points, whether the mice were still untreated, or were treated with HDAd-0 or with HDAd-AI (*Figure 3A*, *Table 1*, and see Supplementary material online, *Table S2*). FPLC analyses of plasma lipoproteins showed increased cholesterol through the entire spectrum of HDL particles of HDAd-AI-treated mice. The pattern of the FPLC profiles and the proportion of human apoA-I associated with each HDL fraction were similar between mice of both genotypes (*Figure 3B* and *C*). Total and non-HDL-cholesterol levels were similar in the four experimental groups through the duration of the study (*Table 1* and see Supplementary material online, *Table S2*). Triglyceride levels were higher in HDAd-AI-treated mice of both genotypes than in HDAd-0-treated mice (*Table 1* and see Supplementary material online, *Table S2*). Increased triglycerides have been observed in other studies following human apoA-I gene transfer, but not in all of them, suggesting that the effect is model and/or diet dependent.[27] However, triglycerides were similarly increased in PLIN2$^{+/+}$/apoE$^{-/-}$ and PLIN2$^{-/-}$/apoE$^{-/-}$ mice.

Next we assessed, by immunohistochemistry, whether higher circulating apoA-I increased apoA-I infiltration in lesions, a necessary step for the subsequent removal of cholesterol from foam cells. As seen in *Figure 4A*, intense apoA-I immunostaining that was relatively uniform through the entire lesion area was observed in atherosclerotic lesions of HDAd-AI-treated mice. Although apoA-I staining was to some extent detectable in lesions of control HDAd-0-treated mice, the staining was generally weaker, with ample areas that were below the detection threshold (*Figure 4A* and *B*). No differences were observed between

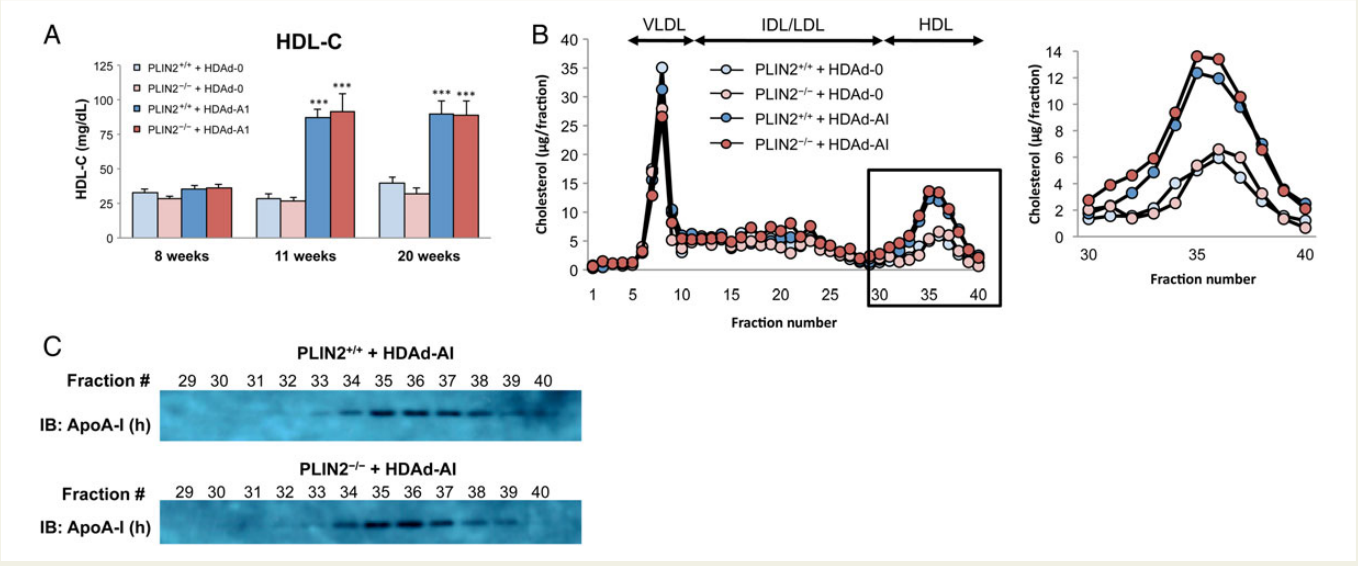

Figure 3 Treatment with HDAd-AI increased HDL-C. (*A*) Plasma HDL-C levels before (8 weeks) and after (11 weeks and 20 weeks) treatment with HDAd-AI or control HDAd-0. ($n = 11–12$). Two-way ANOVA confirmed the significant induction of HDL-C by treatment with HDAd-AI ($P < 0.001$), whereas the PLIN2 genotype did not influence HDL-C levels. ***$P < 0.001$ with respect to HDAd-0-treated PLIN2$^{+/+}$/apoE$^{-/-}$ and PLIN2$^{-/-}$/apoE$^{-/-}$ mice. (*B*) FPLC lipoprotein profiles from pooled plasma at the 20-week time point. (*C*) The content of human apoA-I in the HDL-containing FPLC fractions was assessed by immunoblotting.

Table 1 Body weights and plasma lipids

	HDAd-0		HDAd-AI	
	PLIN2$^{+/+}$/apoE$^{-/-}$	PLIN2$^{-/-}$/apoE$^{-/-}$	PLIN2$^{+/+}$/apoE$^{-/-}$	PLIN2$^{-/-}$/apoE$^{-/-}$
BW (g)	20.1 ± 1.47	20.5 ± 1.30	21.1 ± 0.55	20.9 ± 1.32
Cholesterol (mg/dL)				
Total	492.9 ± 32.00	470.6 ± 26.07	497.5 ± 21.68	486.0 ± 34.95
Non-HDL-C	458.8 ± 32.38	441.0 ± 26.56	408.6 ± 21.25	395.6 ± 32.28
HDL-C	34.1 ± 2.99	29.6 ± 2.16	88.8 ± 5.29***	90.4 ± 8.07***
Total/HDL-C	16.9 ± 2.10	17.4 ± 1.65	6.7 ± 0.65***	5.9 ± 0.55***
Triglyceride (mg/dL)	78.0 ± 3.84	82.9 ± 4.36	135.4 ± 7.23***	147.4 ± 11.46***

Body weights, total cholesterol, non-HDL-cholesterol, and HDL-C values represent post-treatment averages of values obtained at the 11- and 20-week time points. A more detailed table can be found in the online supplemental material (see Supplementary material online, *Table S2*).
***$P < 0.001$ with respect to HDAd-0-treated PLIN2$^{+/+}$/apoE$^{-/-}$ and PLIN2$^{-/-}$/apoE$^{-/-}$ mice, n=11–12 per group.

either basal or post-HDAd-AI apoA-I deposition in lesions between PLIN2$^{+/+}$/apoE$^{-/-}$ and PLIN2$^{-/-}$/apoE$^{-/-}$ mice. Thus, in mice of both genotypes, the hepatic production of human apoA-I was paralleled by similar increases in plasma apoA-I and HDL-C, and by similarly increased apoA-I deposition in lesions.

3.3 Effect of PLIN2 deficiency and elevated apoA-I/HDL-C on atherosclerosis development

The plasma lipid profiles described above illustrate that, while non-HDL-C remained elevated, the hypoalphalipoproteinemia that is also characteristic of apoE$^{-/-}$ mice was corrected by treatment with HDAd-AI.[18] Since HDAd vectors were injected at 8 weeks of age, when atherosclerosis development at the aortic sinus of apoE$^{-/-}$ mice is still undetectable, lesions in HDAd-AI-treated mice primarily developed under higher levels of cholesterol acceptors.[28] At 20 weeks, the average area of lesion involvement at the aortic sinus of HDAd-0-treated PLIN2$^{+/+}$/apoE$^{-/-}$ mice was 260 $\times$ 10^3 μm^2. The average size of lesions of PLIN2-deficient mice and HDAd-AI-treated WT mice was 164 $\times$ 10^3 and 167 $\times$ 10^3 μm^2, respectively (*Figure 5A* and *B*). However, supporting that PLIN2 deficiency and high plasma levels of cholesterol acceptors mutually enhance their atheroprotection, PLIN2$^{-/-}$/apoE$^{-/-}$ mice treated with HDAd-AI presented a much more robust decrease in atherosclerosis development, to an average lesion size of 79 $\times$ 10^3 μm^2 (*Figure 5A* and *B*). Notably, the per cent in lesion size reduction achieved by treatment with HDAd-AI was higher in mice that did not express PLIN2 than in mice that expressed PLIN2: 53% of lesion

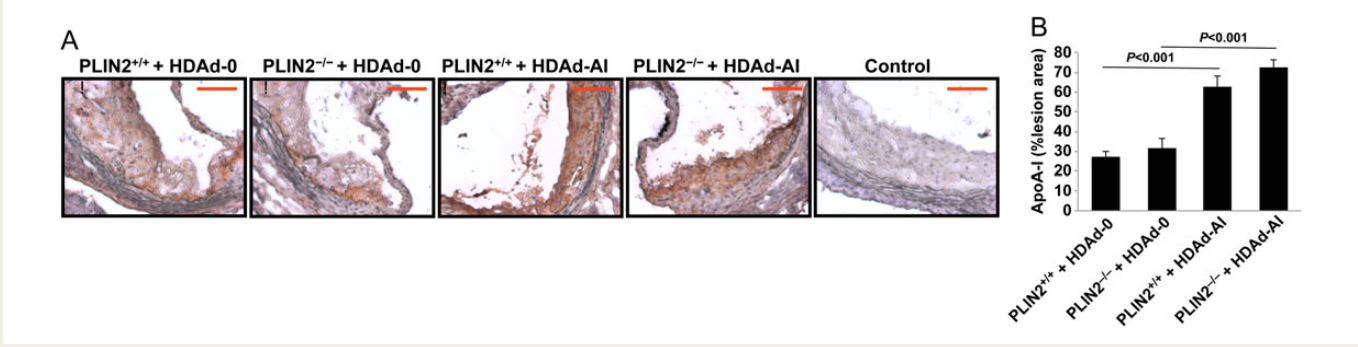

Figure 4 Treatment with HDAd-AI increased apoA-I deposition in atherosclerotic lesions. (*A*) Representative images of atherosclerotic lesions immunostained using an anti-apoA-I antibody that recognizes both mouse and human apoA-I. The sections displayed in this panel are consecutive to the sections displayed in *Figure 7*. Bar = 100 μm. (*B*) Quantification of percentage of lesion area positively stained for apoA-I (n = 7–12). Two-way ANOVA showed a significant effect of treatment with HDAd-AI on apoA-I deposition in lesions ($P < 0.001$), while the PLIN2 genotype had no effect.

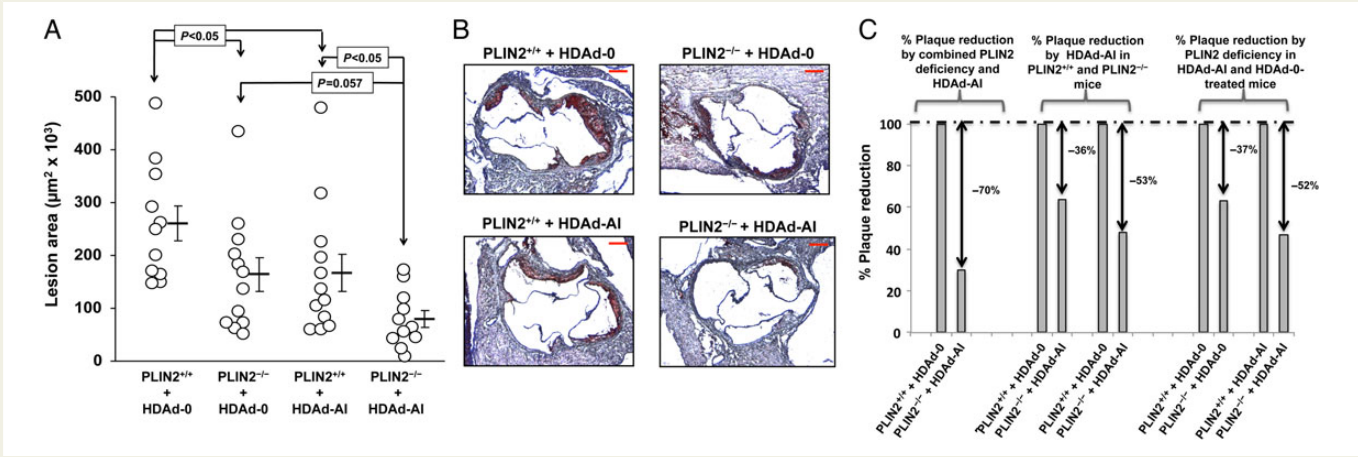

Figure 5 Enhanced atheroprotection by concomitant PLIN2 inactivation and treatment with HDAd-AI. (*A*) Atherosclerotic lesion size at the aortic sinus of PLIN2$^{+/+}$ and PLIN2$^{-/-}$ mice in apoE$^{-/-}$ background that were treated with either HDAd-AI or HDAd-0. The open circles represent individual measurement values. Horizontal bars and error bars represent average $\pm$ SEM, n = 11–12. Two-way ANOVA showed a significant effect of both the PLIN2 genotype ($P < 0.005$) and treatment with HDAd-AI ($P = 0.006$) on atherosclerosis development. The P-values of pairwise comparisons within each factor are shown in the chart. (*B*) Representative images of cross-sections of the aortic sinuses stained with oil red O and counterstained with haematoxylin. (*C*) Relative lesion size reduction by combination of PLIN2 genotype and treatment with HDAd-AI (left chart); relative plaque reduction by HDAd-AI in PLIN2$^{+/+}$/apoE$^{-/-}$ and PLIN2$^{-/-}$/apoE$^{-/-}$ mice (middle chart); and relative effect of PLIN2 ablation on mice that were treated with HDAd-0 or with HDAd-AI (right chart).

reduction in PLIN2$^{-/-}$/apoE$^{-/-}$ mice treated with HDAd-AI vs. 36% reduction in PLIN2$^{+/+}$/apoE$^{-/-}$ mice treated with HDAd-AI. Likewise, the beneficial effect of PLIN2 deficiency was more pronounced in mice with higher levels of acceptors, as PLIN2 deficiency reduced plaque development by 37% in HDAd-0-treated mice and by 52% in HDAd-AI-treated mice (*Figure 5C*).

3.4 PLIN2 deficiency enhances RCT from macrophages to feces and cooperatively reduces lesional lipid content with apoA-I/HDL-C

A fundamental premise for this study is the observation that in cultured macrophages PLIN2, up-regulation decreases cholesterol efflux, whereas PLIN2 deficiency is associated with increased efflux to apoA-I.[2,10] To determine whether lack of PLIN2 also increases cholesterol transport from peripheral cells to liver and feces *in vivo*, we labelled PLIN2$^{+/+}$/apoE$^{-/-}$ and PLIN2$^{-/-}$/apoE$^{-/-}$ PM with ^{3}H-cholesterol, injected the cells into apoE-deficient mice previously treated with HDAd-AI, and traced ^{3}H-cholesterol through plasma, liver, and feces over 48 h. Lack of PLIN2 increased the appearance of ^{3}H-cholesterol in plasma by >100% at the 24 and 48 h time points (*Figure 6A*). The levels of ^{3}H-cholesterol in liver at 48 h were ~1-fold higher in mice injected with PLIN2$^{-/-}$/apoE$^{-/-}$ PM than in mice injected with PLIN2$^{+/+}$/apoE$^{-/-}$ PM, whereas the appearance of ^{3}H-tracer in feces over the 48 h duration of the test was more than three-fold higher in mice injected with PLIN2-deficient macrophages (*Figure 6B* and *C*).

To assess how PLIN2 deficiency and elevated apoA-I/HDL-C affect lipid deposition in arteries, we quantified the average fluorescence intensity in lesions stained with BODIPY 493/503, a fluorescent dye that binds to neutral lipid. As seen in *Figure 6D* and *E*, the staining intensity was weaker in lesions of PLIN2-deficient mice and of HDAd-AI-treated WT mice than in lesions of control empty vector-treated mice, but the lowest intensity values were obtained from lesions of PLIN2$^{-/-}$/apoE$^{-/-}$ mice treated with HDAd-AI. Thus, in addition to reducing the total amount of lipid deposited at the arterial wall, as determined by the reduced area positive for oil red O staining shown in *Figure 5B*, lack of PLIN2 and high apoA-I/HDL-C cumulatively reduced lipid content within lesions. Overall, these results support the observations in cell culture that PLIN2 facilitates cholesterol storage and reduces cholesterol mobilization from foam cells, thus limiting the ability of plasma transporters to clear arterial cholesterol.

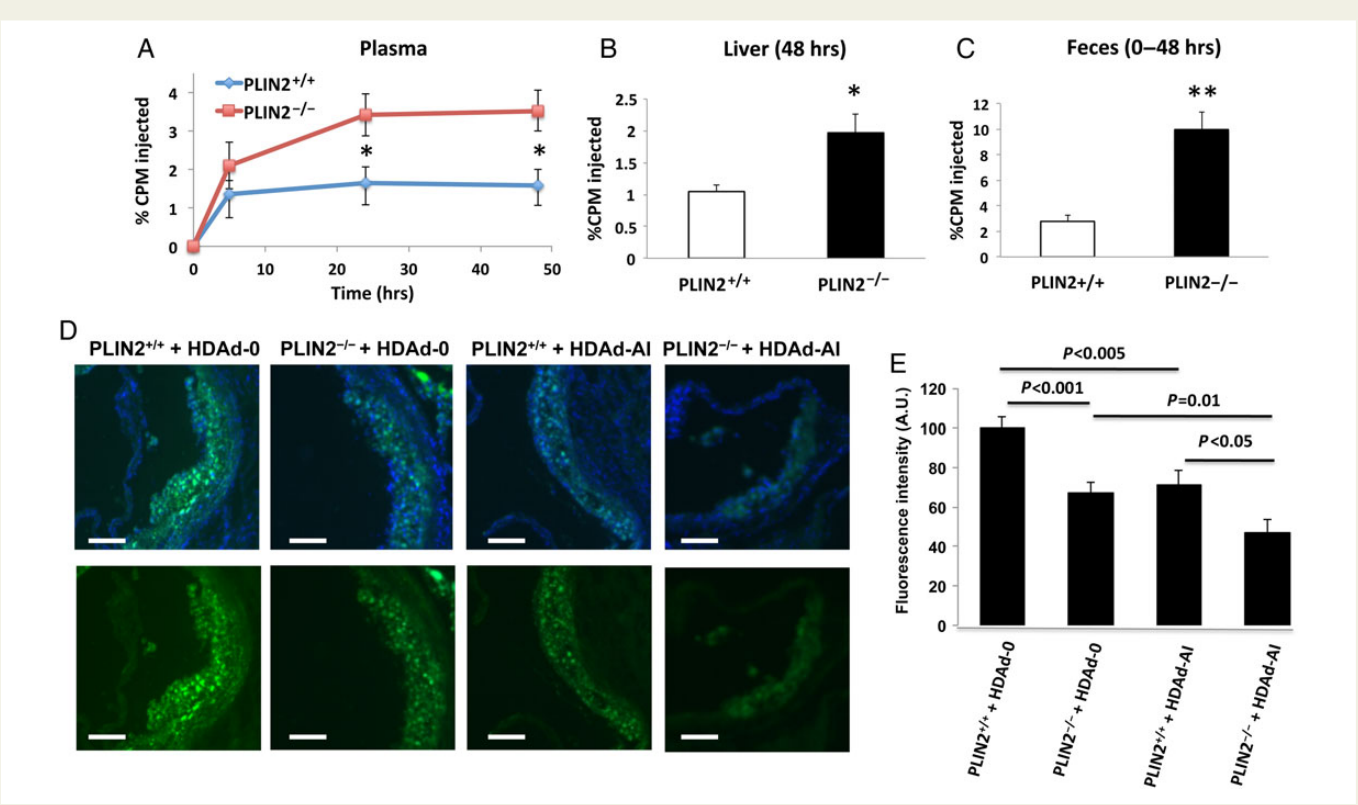

Figure 6 PLIN2 deficiency increases RCT from macrophages to feces and cooperatively reduces lesional lipid content with apoA-I/HDL-C. (*A*–*C*) *In vivo* measurements of RCT. (*A*) Time course of ^{3}H-cholesterol appearance in plasma following injection of ^{3}H-cholesterol-labelled PLIN2$^{+/+}$ or PLIN2$^{-/-}$ PM. (*B*) ^{3}H-cholesterol in liver at 48 h. (*C*) ^{3}H-tracer in feces collected over 48 h. Data are expressed as the percentage of the CPM of ^{3}H-cholesterol tracer injected, $n = 4$. *$P < 0.05$ and **$P < 0.01$ with respect to mice injected with PLIN2$^{+/+}$ PM. (*D* and *E*) Analysis of the effect of PLIN2 ablation and treatment with HDAd-AI on lesional lipid content. (*D*) Representative images of cross-sections of the aortic sinus stained with BODIPY and counterstained with DAPI (upper row) or stained with BODIPY alone (bottom row). Bar = 100 μm. (*E*) Quantification of the intensity of the BODIPY staining in 9–11 lesions per experimental group. By two-way ANOVA, both the PLIN2 genotype and treatment with HDAd-AI significantly reduced the intensity of BODIPY at $P < 0.001$. *P*-values of pairwise comparisons are shown in the chart.

3.5 Induction of plaque stability by elevated apoA-I/HDL-C was enhanced under PLIN2 deficiency

Next, we asked whether the concomitant ablation of PLIN2 and elevation of cholesterol acceptors would affect plaque composition beyond their effect on lipid content. Early atherosclerotic lesions are composed primarily of cholesterol-laden macrophages. The transition from simple fatty streaks to a more complex lesion is characterized by the immigration of smooth muscle cells from the media layer that, in turn, synthesize extracellular matrix proteins, mainly collagen.[1] Thus, we stained cross-sections of the aortic sinus with Masson's trichrome to evaluate the content of collagen and smooth muscle cells and determined macrophage content by immunohistochemistry. As seen in *Figure* 7*A*–*E*, whereas PLIN2 deficiency alone did not significantly affect the relative content of macrophages, smooth muscle cells, and collagen, lesions of mice treated with HDAd-AI presented a moderate but significant reduction in the area of lesion positive for macrophages and a more substantial approximately three-fold increase in collagen content, which paralleled a higher number of smooth muscle cells within lesions. Interestingly, the combination of PLIN2 deficiency and HDAd-AI increased collagen deposition in lesions by ~50% with respect to PLIN2$^{+/+}$/apoE$^{-/-}$ mice treated with HDAd-AI. Given that we did not observe changes in other major plaque features such as the areas of necrotic cores (not shown), and that the relative content of smooth muscle cells and collagen were actually increased but the per cent of area positive for macrophages was lower or remained unchanged, the reduction in total plaque area by both PLIN2 deficiency

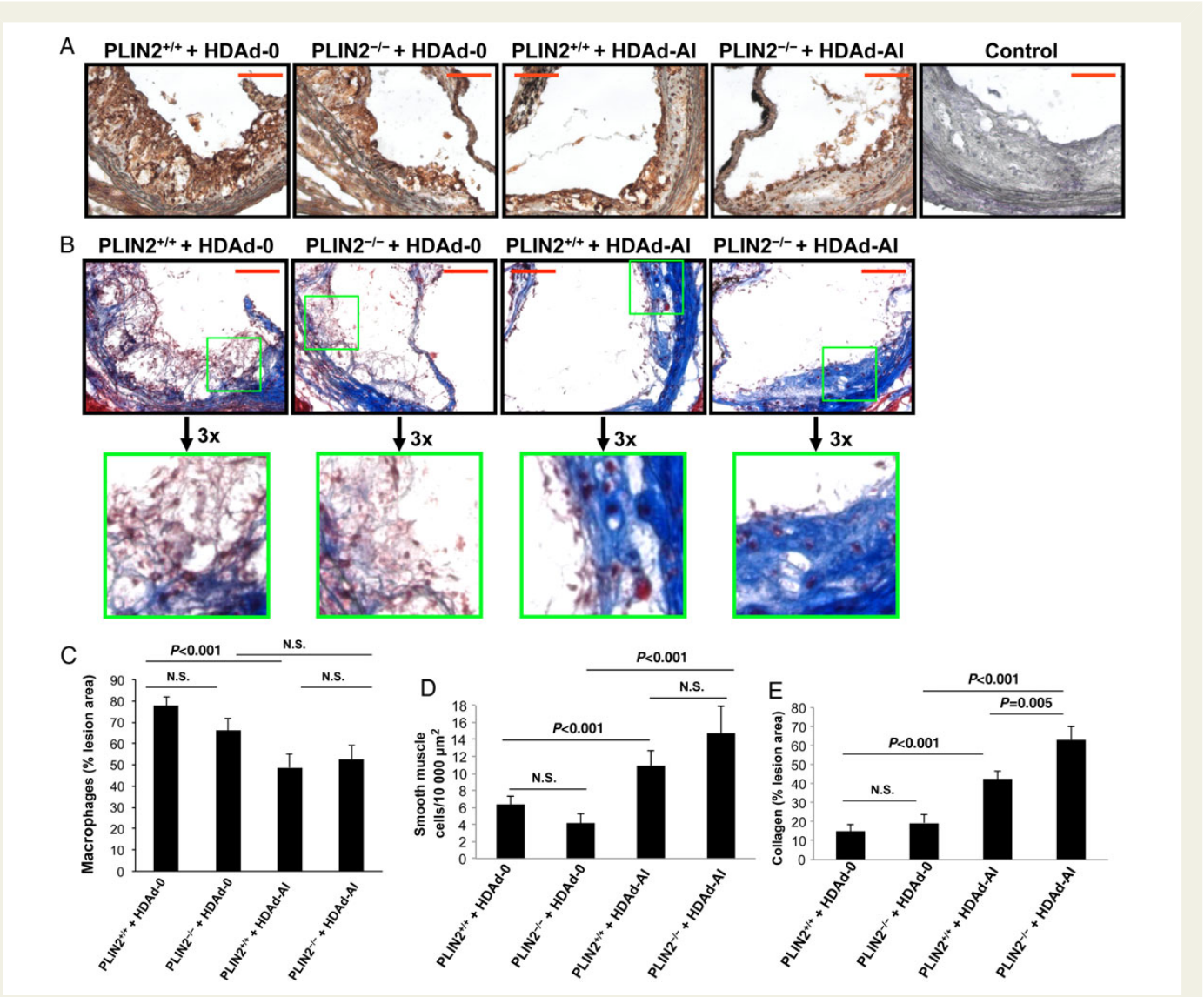

Figure 7 Effects of PLIN2 deficiency and treatment with HDAd-AI on plaque composition. (*A*) Representative images of sections stained with the macrophage marker Mac-3/LAMP-2 (brown colour). (*B*) Representative images of sections stained with Masson's trichrome, which stains collagen blue and smooth muscle cells red. Bar = 100 µm. The sections stained for macrophages and trichrome were consecutive to each other and consecutive to the sections stained for apoA-I displayed in *Figure* 4. (*C*–*E*) Quantification of the Mac-3/LAMP-2 immunoreactive area (*C*), number of smooth muscle cells within the lesions (*D*), and area stained positive for collagen (*E*), ($n = 7$–13). By two-way ANOVA, macrophage and smooth muscle cell content were affected by HDAd-AI treatment ($P < 0.001$ for both), but not by the PLIN2 genotype. Collagen content was affected by both PLIN2 genotype ($P < 0.02$) and by HDAd-AI ($P < 0.001$). *P*-values of pairwise comparisons within factors are shown in the plots.

and treatment with HDAd-AI is likely due to a decrease in the absolute amount of macrophages within the lesions. Thus, although both PLIN2 deficiency and elevated apoA-I/HDL-C reduced lipid content in lesions, a more stable plaque phenotype with relatively less macrophages and increased smooth muscle cells and collagen was primarily associated with elevated apoA-I and HDL-C. However, the effect of HDAd-AI on collagen deposition in lesions was stronger in PLIN2$^{-/-}$/apoE$^{-/-}$ mice.

4. Discussion

The aetiology of atherosclerosis is intrinsically linked to cholesterol accumulation at the arterial wall, caused by an imbalance between deposition and removal.[12] To develop novel approaches to reduce arterial cholesterol as a way of ameliorating atherosclerosis development, it will be critical to advance our understanding on how RCT from arteries is regulated. A central step in the process involves efflux of cholesterol from foam cells to extracellular acceptors, which subsequently return cholesterol to the liver. The notion that promoting RCT is a valid strategy for therapeutic purposes has been supported by studies in animal models of atherosclerosis showing an anti-atherogenic response both when proteins in foam cells were targeted to facilitate efflux (reviewed in[12,29]) or, as reviewed in the introduction, when the plasma concentrations of cholesterol acceptors were increased. Given that both the ability of foam cells to efflux cholesterol and the ability of the extracellular milieu to accept it might be limiting factors in RCT, we hypothesized that atheroprotection would be enhanced by conjointly inactivating PLIN2 to increase the foam cell's ability to efflux cholesterol and increasing the circulating levels of apoA-I and HDL-C. Supporting this hypothesis, this study shows substantially reduced atherosclerosis development in PLIN2-deficient mice that were treated with HDAd-AI to increase plasma apoA-I and HDL-C than that achieved by PLIN2 deficiency alone or by treating WT mice with HDAd-AI (*Figure 8*).

Long-standing epidemiological studies have shown that HDL-C levels are strong, independent, inverse predictors of cardiovascular events. Large population studies showed that as little as a 1 mg/dL increment in HDL-C decreased the risk of coronary heart disease by 2% in men and by 3% in women.[30] However, recent attempts at increasing HDL-C have brought into question whether simply raising HDL-C is sufficient to achieve atheroprotection, denoting the need to also focus on how to improve the functional capacity of HDL.[31,32] In this study, treatment with HDAd-AI corrected hypoalphalipoproteinaemia in apoE$^{-/-}$ mice, raising HDL-C to levels similar or slightly more elevated than that seen in humans in the higher percentile values.[26] While the hepatic production of both mouse and human apoA-I, the circulating levels of apoA-I and HDL-C, and apoA-I deposition in lesions were similar between mice that did or did not express PLIN2, the per cent of lesion size reduction associated with increased apoA-I/HDL-C was higher in PLIN2-deficient mice than in their PLIN2-expressing littermates. Likewise, the relative atheroprotection associated with PLIN2 deficiency was increased upon treatment with HDAd-AI. Overall, these data suggest that the atheroprotection achieved by raising plasma

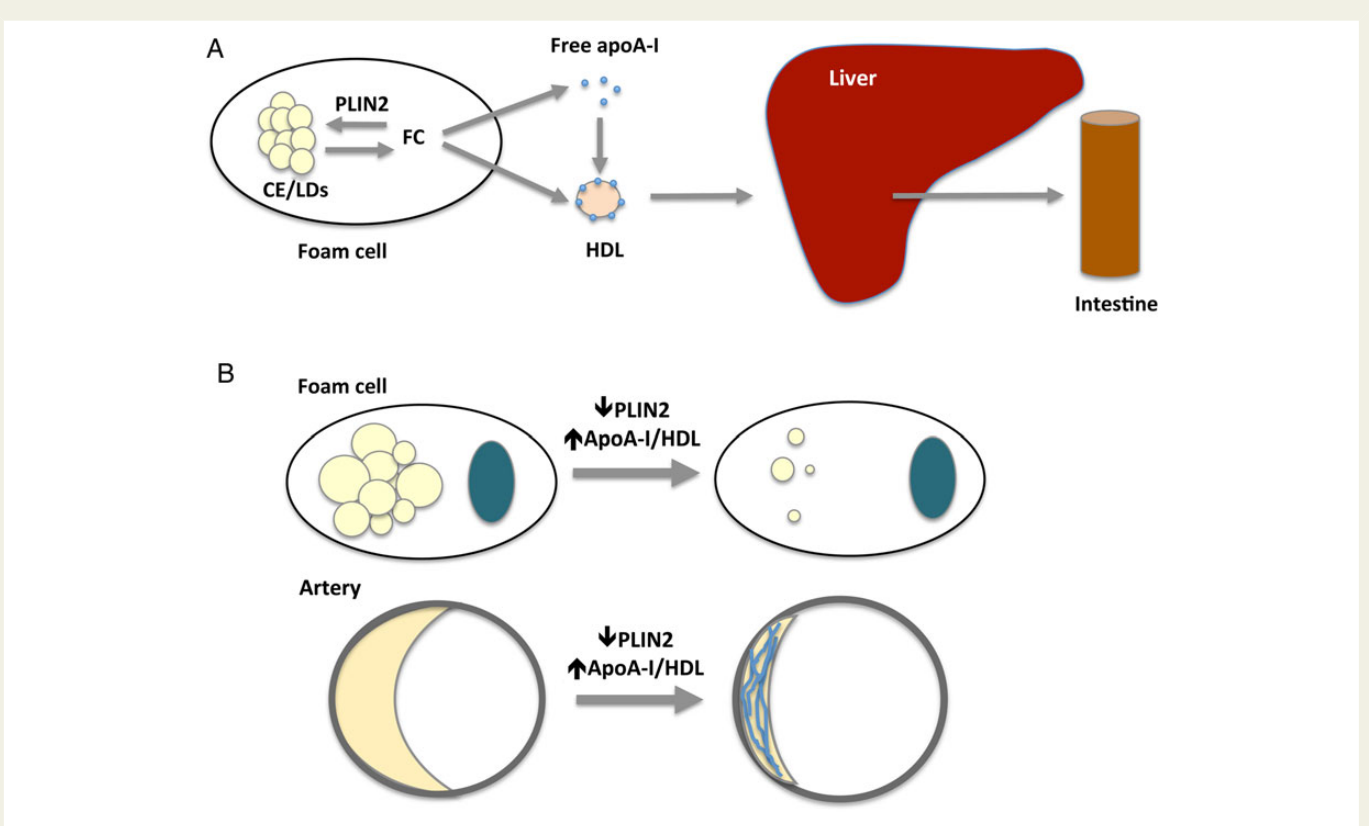

Figure 8 (*A*) Roles of PLIN2 and apoA-I/HDL in RCT. By promoting compartmentalization of intracellular cholesterol as CE in LDs, PLIN2 limits the amount cholesterol available to feed efflux effectors, therefore reducing the overall RCT from foam cells to feces. CE, cholesterol ester; FC, free cholesterol. (*B*) Concomitantly targeting PLIN2 and increasing plasma apoA-I/HDL-C significantly enhances the ability of the individual interventions to remove cholesterol from foam cells, increases atheroprotection, and promotes plaque stability.

apoA-I and HDL-C can be enhanced by concomitantly targeting foam cell proteins involved in cholesterol homeostasis to facilitate efflux, and *vice versa*.

The notion that PLIN2 ablation and apoA-I/HDL-C cooperatively prevent cholesterol deposition in foam cells and arteries is supported *in vitro* by studies showing that the CE depots in macrophages that lack PLIN2 can be further reduced by supplementing the culture media with apoA-I and, *in vivo*, by a substantial reduction in the absolute area of oil red O staining in the arterial intima, and by the lower intensity of BODIPY staining observed in lesions of PLIN2-deficient mice treated with HDAd-AI. *In vivo* RCT assays showed that the increased cholesterol efflux seen under PLIN2 deficiency is not restricted to cultured cells, as loss of PLIN2 in macrophages enhanced RCT from macrophages to plasma, liver, and feces. However, both elevated apoA-I/HDL-C could also have influenced lesion development by mechanisms unrelated to their ability to promote RCT from atherosclerotic lesions. For example, other putatively atheroprotective properties of HDL include antioxidant, anti-inflammatory, and anti-thrombotic properties.[13] Regarding PLIN2, the protein is expressed quite ubiquitously, which could be give rise to systemic effects that could be either favourable or unfavourable. Systemic untoward effects related to PLIN2 deficiency would almost necessarily imply that for therapeutic purposes, PLIN2 would have to be selectively targeted in macrophages, which would considerably constrain the potential of targeting PLIN2. However, although it was reported that PLIN2 up-regulation in skeletal muscle improved muscle insulin resistance,[7] insulin levels and the response to glucose tolerance tests were similar in mice that did or did not express PLIN2.[33] In obese mice, global PLIN2 deficiency was shown to improve glucose tolerance and insulin sensitivity in both liver and muscle.[34] Other putatively beneficial effects related to PLIN2 deficiency could include protection against hepatosteatosis and against diet-induced obesity.[6,35] Nevertheless, arguing against a significant impact of systemic PLIN2 ablation on atherosclerosis development, previously we demonstrated that global PLIN2 deficiency and loss of PLIN2 in bone marrow-derived cells protected apoE$^{-/-}$ mice against atherosclerosis to a similar extent.[2]

Interestingly, whereas both PLIN2 deficiency and increased apoA-I/HDL-C decreased lipid content and had a similar effect on plaque reduction, morphological analyses revealed differences between lesions of mice deficient in PLIN2 and those of mice treated with HDAd-AI, with the latter having a moderate reduction in macrophages, but increased smooth muscle cells and collagen content. The combination of PLIN2 deficiency and HDAd-AI treatment further increased collagen deposition. Lesion composition can significantly impact the likelihood of plaque rupture, which causes most clinically relevant cardiovascular events. While macrophage-rich areas within lesions are prone to rupture, collagen deposition is considered a hallmark of plaque stability.[36,37] Thus, the lesions of HDAd-AI-treated mice presented a more stable morphology. Our findings are consistent with previous reports showing lesions with a more favourable phenotype, often containing more collagen, following plasma elevations in apoA-I and HDL-C.[18,20,25,27,38,39] Given that lesions of PLIN2-deficient mice also contain less lipid, it is unlikely that the reduction in lipid content mediated by apoA-I and HDL-C is the only cause of the changes in lesion composition. Indicating that arterial lipid content is not always inversely related to markers of plaque stability, combined deletion of the cholesterol transporters ABCA1 and ABCG1 led to extreme foam cell formation but did not change lesion composition. Additionally, ABCA1 up-regulation was not associated with changes in collagen deposition, or it actually decreased collagen deposition, which could be indicative of less advanced lesions.[40–42] Although the molecular mechanisms leading to the favourable remodelling of atherosclerotic lesions have yet to be elucidated, assuming that atherosclerosis development cannot be fully prevented, it seems evident that the development of small and highly stable lesions like that seen in HDAd-AI-treated PLIN2-deficient mice would be very desirable.

In conclusion, this study reveals a mutually beneficial relationship between PLIN2 inactivation and circulating apoA-I and HDL-C in ameliorating atherogenesis and in promoting plaque stability. It is increasingly clear that the functional capacity of apoA-I and HDL-C to remove cholesterol from arteries is not only dependent on their concentration.[32] The data presented here illustrate that the anti-atherogenic potential of therapies that raise HDL-C can be enhanced by targeting cellular components to mobilize cholesterol from foam cells.

Supplementary material

Supplementary material is available at *Cardiovascular Research* online.

Acknowledgements

We thank the MMC Core at BCM under DRC for lipid profiling.

Conflict of interest: none declared.

Funding

This work was supported by NIH grants (HL104251 to A.P.) and (HL-51586/DK105527 to L.C.). Y.H.G. was partly supported by an American Heart Association Scientist Development Grant (14SDG19690016). L.C. was also supported by the Betty Rutherford Chair for Diabetes Research from St Luke's Episcopal Hospital and Baylor College of Medicine. This work was partly supported by the Diabetes and Endocrinology Research Center (P30 DK079638) at Baylor College of Medicine.

References

1. Glass CK, Witztum JL. Atherosclerosis: the road ahead. *Cell* 2001;**104**:503–516.
2. Paul A, Chang BH, Li L, Yechoor VK, Chan L. Deficiency of adipose differentiation-related protein impairs foam cell formation and protects against atherosclerosis. *Circ Res* 2008;**102**:1492–1501.
3. Kimmel AR, Brasaemle DL, Andrews-Hill M, Sztalryd C, Londos C. Adoption of PERILIPIN as a unifying nomenclature for the mammalian PAT-family of intracellular lipid storage droplet proteins. *J Lipid Res* 2010;**51**:468–471.
4. Xu G, Sztalryd C, Lu X, Tansey JT, Gan J, Dorward H, Kimmel AR, Londos C. Post-translational regulation of adipose differentiation-related protein by the ubiquitin/proteasome pathway. *J Biol Chem* 2005;**280**:42841–42847.
5. Straub BK, Gyoengyoesi B, Koenig M, Hashani M, Pawella LM, Herpel E, Mueller W, Macher-Goeppinger S, Heid H, Schirmacher P. Adipophilin/perilipin-2 as a lipid droplet-specific marker for metabolically active cells and diseases associated with metabolic dysregulation. *Histopathology* 2013;**62**:617–631.
6. Chang BH-J, Li L, Paul A, Taniguchi S, Nannegari V, Heird WC, Chan L. Protection against fatty liver but normal adipogenesis in mice lacking adipose differentiation-related protein. *Mol Cell Biol* 2006;**26**:1063–1076.
7. Bosma M, Hesselink MKC, Sparks LM, Timmers S, Ferraz MJ, Mattijssen F, van Beurden D, Schaart G, de Baets MH, Verheyen FK, Kersten S, Schrauwen P. Perilipin 2 improves insulin sensitivity in skeletal muscle despite elevated intramuscular lipid levels. *Diabetes* 2012;**61**:2679–2690.
8. Imanishi Y, Sun W, Maeda T, Maeda A, Palczewski K. Retinyl ester homeostasis in the adipose differentiation-related protein-deficient retina. *J Biol Chem* 2008;**283**:25091–25102.
9. Dahlhoff M, Camera E, Picardo M, Zouboulis CC, Chan L, Chang BH-J, Schneider MR. PLIN2, the major perilipin regulated during sebocyte differentiation, controls sebaceous lipid accumulation in vitro and sebaceous gland size in vivo. *Bioch Biophys Acta-Gen Subj* 2013;**1830**:4642–4649.
10. Larigauderie G, Furman C, Jaye M, Lasselin C, Copin C, Fruchart JC, Castro G, Rouis M. Adipophilin enhances lipid accumulation and prevents lipid efflux from THP-1 macrophages: potential role in atherogenesis. *Arterioscler Thromb Vasc Biol* 2004;**24**:504–510.
11. Son SH, Goo YH, Chang BH, Paul A. Perilipin 2 (PLIN2)-deficiency does not increase cholesterol-induced toxicity in macrophages. *PLoS ONE* 2012;**7**:e33063.

12. Cuchel M, Rader DJ. Macrophage reverse cholesterol transport: key to the regression of atherosclerosis? *Circulation* 2006;**113**:2548–2555.
13. Tall AR. Cholesterol efflux pathways and other potential mechanisms involved in the athero-protective effect of high density lipoproteins. *J Intern Med* 2008;**263**:256–273.
14. Gordon DJ, Rifkind BM. High-density lipoprotein—the clinical implications of recent studies. *N Engl J Med* 1989;**321**:1311–1316.
15. Plump AS, Scott CJ, Breslow JL. Human apolipoprotein A-I gene expression increases high density lipoprotein and suppresses atherosclerosis in the apolipoprotein E-deficient mouse. *Proc Natl Acad Sci USA* 1994;**91**:9607–9611.
16. Pászty C, Maeda N, Verstuyft J, Rubin EM. Apolipoprotein AI transgene corrects apolipoprotein E deficiency-induced atherosclerosis in mice. *J Clin Invest* 1994;**94**:899–903.
17. Tangirala RK, Tsukamoto K, Chun SH, Usher D, Puré E, Rader DJ. Regression of atherosclerosis induced by liver-directed gene transfer of apolipoprotein A-I in mice. *Circulation* 1999;**100**:1816–1822.
18. Rong JX, Li J, Reis ED, Choudhury RP, Dansky HM, Elmalem VI, Fallon JT, Breslow JL, Fisher EA. Elevating high-density lipoprotein cholesterol in apolipoprotein E-deficient mice remodels advanced atherosclerotic lesions by decreasing macrophage and increasing smooth muscle cell content. *Circulation* 2001;**104**:2447–2452.
19. Pastore L, Belalcazar LM, Oka K, Cela R, Lee B, Chan L, Beaudet AL. Helper-dependent adenoviral vector-mediated long-term expression of human apolipoprotein A-I reduces atherosclerosis in apo E-deficient mice. *Gene* 2004;**327**:153–160.
20. Belalcazar LM, Merched A, Carr B, Oka K, Chen KH, Pastore L, Beaudet A, Chan L. Long-term stable expression of human apolipoprotein A-I mediated by helper-dependent adenovirus gene transfer inhibits atherosclerosis progression and remodels atherosclerotic plaques in a mouse model of familial hypercholesterolemia. *Circulation* 2003;**107**:2726–2732.
21. Oka K, Belalcazar LM, Dieker C, Nour EA, Nuno-Gonzalez P, Paul A, Cormier S, Shin JK, Finegold M, Chan L. Sustained phenotypic correction in a mouse model of hypoalphalipoproteinemia with a helper-dependent adenovirus vector. *Gene Ther* 2007;**14**:191–202.
22. Paigen B, Morrow A, Holmes PA, Mitchell D, Williams RA. Quantitative assessment of atherosclerotic lesions in mice. *Atherosclerosis* 1987;**68**:231–240.
23. Goo Y-H, Son S-H, Kreienberg PB, Paul A. Novel lipid droplet–associated serine hydrolase regulates macrophage cholesterol mobilization. *Arterioscler Thromb Vasc Biol* 2014;**34**:386–396.
24. Zhang Y, Da Silva JR, Reilly M, Billheimer JT, Rothblat GH, Rader DJ. Hepatic expression of scavenger receptor class B type I (SR-BI) is a positive regulator of macrophage reverse cholesterol transport in vivo. *J Clin Invest* 2005;**115**:2870–2874.
25. Rayner KJ, Sheedy FJ, Esau CC, Hussain FN, Temel RE, Parathath S, van Gils JM, Rayner AJ, Chang AN, Suarez Y, Fernandez-Hernando C, Fisher EA, Moore KJ. Antagonism of miR-33 in mice promotes reverse cholesterol transport and regression of atherosclerosis. *J Clin Invest* 2011;**121**:2921–2931.
26. Schaefer EJ, Lamon-Fava S, Ordovas JM, Cohn SD, Schaefer MM, Castelli WP, Wilson PW. Factors associated with low and elevated plasma high density lipoprotein cholesterol and apolipoprotein A-I levels in the Framingham Offspring Study. *J Lipid Res* 1994;**35**:871–882.
27. Van Craeyveld E, Gordts S, Nefyodova E, Jacobs F, De Geest B. Regression and stabilization of advanced murine atherosclerotic lesions: a comparison of LDL lowering and HDL raising gene transfer strategies. *J Mol Med* 2011;**89**:555–567.
28. Reddick RL, Zhang SH, Maeda N. Atherosclerosis in mice lacking apo E. Evaluation of lesional development and progression. *Arterioscler Thromb* 1994;**14**:141–147.
29. Ouimet M, Marcel YL. Regulation of lipid droplet cholesterol efflux from macrophage foam cells. *Arterioscler Thromb Vasc Biol* 2012;**32**:575–581.
30. Gordon DJ, Probstfield JL, Garrison RJ, Neaton JD, Castelli WP, Knoke JD, Jacobs DR, Bangdiwala S, Tyroler HA. High-density lipoprotein cholesterol and cardiovascular disease. Four Prospective American Studies. *Circulation* 1989;**79**:8–15.
31. Tuteja S, Rader DJ. High-density lipoproteins in the prevention of cardiovascular disease: changing the paradigm. *Clin Pharmacol Ther* 2014;**96**:48–56.
32. Khera AV, Cuchel M, de la Llera-Moya M, Rodrigues A, Burke MF, Jafri K, French BC, Phillips JA, Mucksavage ML, Wilensky RL, Mohler ER, Rothblat GH, Rader DJ. Cholesterol efflux capacity, high-density lipoprotein function, and atherosclerosis. *N Engl J Med* 2011;**364**:127–135.
33. Carr RM, Peralta G, Yin X, Ahima RS. Absence of perilipin 2 prevents hepatic steatosis, glucose intolerance and ceramide accumulation in alcohol-fed mice. *PLoS ONE*. 2014;**9**:e97118.
34. Chang BH-J, Li L, Saha P, Chan L. Absence of adipose differentiation related protein upregulates hepatic VLDL secretion, relieves hepatosteatosis, and improves whole body insulin resistance in leptin-deficient mice. *J Lipid Res* 2010;**51**:2132–2142.
35. McManaman JL, Bales ES, Orlicky DJ, Jackman M, MacLean PS, Cain S, Crunk AE, Mansur A, Graham CE, Bowman TA, Greenberg AS. Perilipin-2-null mice are protected against diet-induced obesity, adipose inflammation, and fatty liver disease. *J Lipid Res* 2013;**54**:1346–1359.
36. Carr SC, Farb A, Pearce WH, Virmani R, Yao JST. Activated inflammatory cells are associated with plaque rupture in carotid artery stenosis. *Surgery* 1997;**122**:757–763.
37. Rekhter MD. Collagen synthesis in atherosclerosis: too much and not enough. *Cardiovasc Res* 1999;**41**:376–384.
38. Choudhury RP, Rong JX, Trogan E, Elmalem VI, Dansky HM, Breslow JL, Witztum JL, Fallon JT, Fisher EA. High-density lipoproteins retard the progression of atherosclerosis and favorably remodel lesions without suppressing indices of inflammation or oxidation. *Arterioscler Thromb Vasc Biol* 2004;**24**:1904–1909.
39. Reimers GJ, Jackson CL, Rickards J, Chan PY, Cohn JS, Rye K-A, Barter PJ, Rodgers KJ. *Inhibition of rupture of established atherosclerotic plaques by treatment with apolipoprotein A-I. Cardiovasc Res* 2011;**91**:37–44.
40. Out R, Hoekstra M, Habets K, Meurs I, de Waard V, Hildebrand RB, Wang Y, Chimini G, Kuiper J, Van Berkel TJ, Van Eck M. Combined deletion of macrophage ABCA1 and ABCG1 leads to massive lipid accumulation in tissue macrophages and distinct atherosclerosis at relatively low plasma cholesterol levels. *Arterioscler Thromb Vasc Biol* 2008;**28**:258–264.
41. Van Eck M, Singaraja RR, Ye D, Hildebrand RB, James ER, Hayden MR, Van Berkel TJC. Macrophage ATP-binding cassette transporter A1 overexpression inhibits atherosclerotic lesion progression in low-density lipoprotein receptor knockout mice. *Arterioscler Thromb Vasc Biol* 2006;**26**:929–934.
42. Fu Y, Mukhamedova N, Ip S, D'Souza W, Henley Katya J, DiTommaso T, Kesani R, Ditiatkovski M, Jones L, Lane Rachael M, Jennings G, Smyth Ian M, Kile Benjamin T, Sviridov D. ABCA12 regulates ABCA1-dependent cholesterol efflux from macrophages and the development of atherosclerosis. *Cell Metab* 2013;**18**:225–238.